# Spectrally-selective Photovoltaics via Photonic Band Engineering in Absorbing Media

Arlene Chiu, Botong Qiu, Yida Lin, Ebuka S. Arinze, Lulin Li, and Susanna M. Thon
Department of Electrical and Computer Engineering, Johns Hopkins University, Baltimore, MD, 21218,
USA

Abstract — Spectral selectivity is of interest for many photovoltaic applications, such as in multijunction and transparent solar cells, where wavelength-selectivity of the photoactive material is necessary. We investigate using artificial photonic band engineering as a method for achieving spectral selectivity in an absorbing material such as PbS CQD thin films. Using FDTD simulations, we find that a CQD-based photonic crystal (CQD-PC) is able to maintain its photonic band structure, including the existence of a reduced photonic density of states, in the presence of weak material absorption. This shows that CQD-PCs are a promising material for photovoltaic applications that require spectral selectivity.

Index Terms — spectral selectivity, photonic crystals, colloidal quantum dots, thin film material, photovoltaics,

## I. Introduction

Spectral selectivity has many applications in optoelectronics such as in optical imaging [1], [2], target recognition [3], chemical detection [3], [4], and solar energy harvesting [5], but is difficult to achieve for typical traditional semiconductors that absorb at all energies above their band gaps. Spectral selectivity is of particular interest for multijunction and transparent that require materials photovoltaics with transparency windows [5]. Solutions to this problem currently involve using external filters for photodetectors [4], adding both cost and complexity to the system, as well as empirically controlling the thickness of the absorbing layers in tandem solar cells to achieve current-matching, which usually sacrifices photocurrent output [6]. Spectral selectivity for heat management is usually achieved by attempting to reflect unwanted wavelengths that would be parasitically absorbed in the contacts or other device layers [7]. Here we propose using photonic crystals to produce controlled spectral selectivity within the absorbing medium itself, through engineering the photonic band structure to directly control the wavelengthdependent absorption, reflection and transmission.

Photonic crystals (PCs) are composed of materials with periodic variations in their dielectric functions that can potentially exhibit photonic band gaps, ranges of frequencies where photons are forbidden to propagate. This enables PCs to be used as a mechanism to manipulate light flow, such as in optical communications [8], computing [9], and optoelectronics [10]. Most of these applications use PCs with the photonic band gap in the non-absorbing wavelength region of the materials, below the electronic band where the material behaves as a simple dielectric, although tuning the frequency location of the

photonic band gap can be done by adjusting the scale of the PC [11]. Positioning the photonic band gap of a PC in an absorbing material is atypical due to optical absorption being seen as a loss mechanism in many applications. However, photovoltaic applications rely heavily on semiconductor absorption as a crucial operation mechanism. Therefore, we propose using photonic band engineering within the absorbing material as a potential new spectral tuning mechanism.

Spectral-selectivity is of particular interest with regards to color-tuned materials with controlled transparency windows for multijunction and transparent photovoltaics. Infrared (IR) sensitive small-bandgap semiconductors absorb strongly at all energies above their band gap. Materials such as organic semiconductors [12] typically have finite-bandwidth absorption in the visible and UV range, but IR-only materials are very rare. Usually, for IR-sensitive materials to be incorporated into multijunction solar cells, they must be positioned at the back of the cell to allow for absorption of the visible wavelengths by the front cell to occur. In this scenario, the thickness of both cells must be finely tuned to achieve current matching. The ideal material to incorporate multijunction functionality into current single junction photovoltaic technology would have a tunable and finite bandwidth absorption profile and offer flexibility for device design and current matching by allowing the IR material to be placed on either side of the visible cell.

The concept of using the photonic band structure in a slabtype PC to control the external absorption, reflection and transmission spectrum is illustrated in Fig 1. A system composed of a 2D PC "slab" with a periodic array of air holes drilled in a semiconductor is presented in the left portion of Fig. 1. The "out-of-plane", incident, reflected and transmitted fields interact with the "in-plane" resonant field, with properties that are determined by the PC structure. The "in-plane" fields and band structure couple to the "out-of-plane" transmission and reflection spectra at the γ point of the Brillouin Zone, shown in the right portion of Fig 1. The transmitted and reflected fields directly couple to the incident field and simultaneously indirectly couple to the radiating mode of the PC slab, which can be explained by temporal-coupled wave theory [13], [14], [15]. Specifically, hypothetical reflection and transmission spectra at normal incidence are shown alongside a hypothetical (generic) in-plane photonic band diagram for a structure such as the one shown on the left side of the figure to demonstrate the coupling between the in-plane photonic bands and the outof-plane reflection and transmission spectra. The transmission

and reflection profiles are composed of smooth varying background that resembles a Fabry-Perot interference spectrum [16], with sharp and asymmetric resonance features on top. The coupling between the incident wave and the photonic bands that share a lateral wave-vector creates resonance features in the transmission and reflection spectra of the slab. This phenomenon produces the potential for tuning the "out-of-plane" spectral selectivity through adjusting the band structure of the PC slab to accomplish the desired absorption, reflection, and transmission profiles.

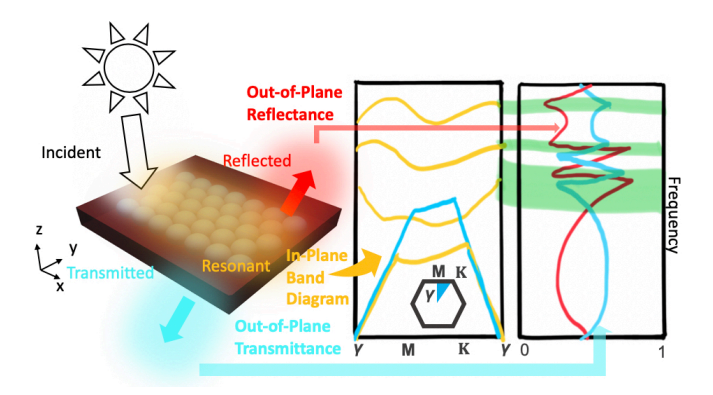


Fig. 1. Schematic of a generic 2D "slab" photonic crystal depicting the spectral tuning concept (left). Broadband incident light (white in color), strongly couples to the "in-plane" resonant modes (yellow), producing spectrally-selective "out-of-plane" reflectivity (red) and transmissivity (blue). A hypothetical photonic band diagram for a generic slab structure is sketched in the middle panel. The photonic bands are shown in yellow, with the light line in blue. The inset is the Brillouin zone for a 2D triangular lattice photonic crystal. The "out-of-plane" reflectivity (red) and transmissivity (blue) spectra at normal incidence are shown in the right panel. The green stripes highlight the direct correlations (coupling) between the sharp resonance features for the transmittance and reflectance spectra and the photonic bands at the  $\gamma$ -point.

In this work, we use finite-difference time domain (FDTD) simulations to calculate the photonic band structure of a PbS colloidal quantum dot (CQD) thin film-based photonic crystal [17], that strongly absorbs in the infrared and transmits visible light more strongly than its non-structured counterpart. We also quantify the effects of material absorption on the photonic band structure. This type of material could potentially be used as a flexible infrared layer to achieve current-matching in a tandem solar cell.

## II. SIMULATIONS

To study the photonic bands of a PC formed in an absorbing material, we based our simulations on a previously experimentally demonstrated structure [17]. The structure of interest is composed of a monolayer triangular lattice array of polystyrene spheres, which serve as the low-index material, [17] infiltrated with absorbing PbS colloidal quantum dots, chosen due to their infrared responsivity, facile solution

processability, and previous application in solar cells [18], [19].

Using FDTD simulations, we can probe the effect of CQD material absorption on the photonic band structure by artificially setting the imaginary part of the dielectric constant  $(\epsilon_{\rm I})$  to zero and the real part  $(\epsilon_{\rm R})$  to a constant, equivalent to adjusting the real and imaginary parts of the refractive index (n,k). In this test-case model, dispersion is not explicitly considered due to the resulting difficulty in satisfying the Kramers-Kronig relations [20]. We determine the photonic band structure of our materials by calculating the frequencies of the modes that can exist in the structure beyond the initial transient phase, either with or without material absorption. We are then able to calculate the photonic band structure by using a broadband excitation source to ensure that all modes of interest are excited and collecting time-resolved field data using randomly distributed time monitors. Destructive interference causes rapid decay of non-resonant fields, while excited modes of the structure resonate with varying decay rates for the duration of the simulation. The frequencies of these modes are extracted using fast Fourier transform (FFT).

Details of the FDTD simulation method for band structure calculations [21] are as follows: A simulation volume of an integer number of unit cells of the 2D periodic structure is considered, and the volume is extended in the z-direction above and below the slab symmetrically for approximately 10 lattice constants. Bloch boundary conditions are applied for the x and y (in-plane) directions and perfectly matched layers (PMLs) are used for the z-direction with symmetric or anti-symmetric boundary conditions, corresponding respectively to even (TElike) or odd (TM-like) modes. Identical broadband dipole sources are randomly distributed throughout the simulation space to excite the various modes. Conformal meshing is used at the material interfaces, incorporating Maxwell's integral equations to account for structural variations within a single mesh cell. The loaded time signals from each time monitor for each field component are apodized with a Gaussian-shaped window function to focus on the time signal following the source pulse injection and before the simulation time ends. The resulting FFTs of the apodized signals comprise a spectrum consisting of peaks corresponding to the resonant modes associated with the allowed photonic bands. For each field component, the energy spectra of the Fourier-transformed time signals of every time monitor are summed to ensure the identification of all of the resonant frequencies. This is to account for any time monitors that may have been randomly placed at the node of a mode. The simulations are repeated for each Bloch vector value (K), and frequency peaks for each K that meet the threshold tolerance are kept.

In our simulation, we use a slab thickness (t) of 250 nm, a lattice constant (a) of 250 nm, and two different sphere diameters of d = 250 nm and d = 200 nm to demonstrate a close-packed and a slightly etched sphere lattice, respectively. The model structure is shown in Fig. 2(d). We use experimental

values for the real and imaginary parts of the dielectric constant for the CQD medium and a (real) dielectric constant of 1.6 for the latex spheres. A (real) dielectric constant of 2.6 is chosen as representative of the average of the CQD medium in the frequency range of interest and held constant to simulate the band structure for the control case of no material absorption.

## III. RESULTS

A diagram of the simulated structure is shown in Fig. 2(d). The simulated photonic band structure for the non-absorbing close-packed case with both even and odd modes is shown in the top left panel of Fig. 2(a), followed by the results for a close-packed (d = 250 nm) CQD-PC slab with full dispersion in the refractive index model in Fig. 2(b). In Fig. 2(c), the photonic band structure of an etched (d = 200 nm) CQD-PC with full dispersion is shown. In Fig. 2(e) the real and imaginary parts of the full refractive index model for the CQD material are plotted.

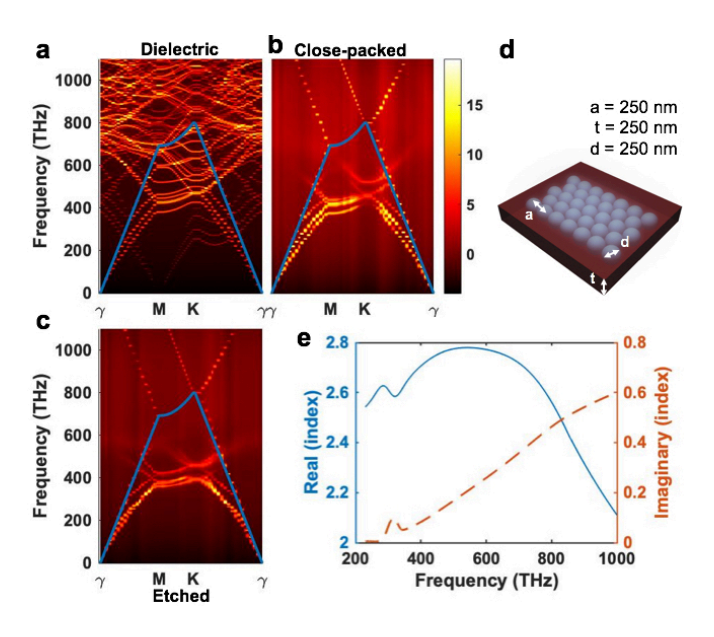


Fig. 2. (a) FDTD-calculated photonic band diagrams for the structure shown in (d) with d=250 nm for the case of no absorption (b) the case with full material dispersion, and (c) the case with full material dispersion and d=200 nm. (d) Model of the simulated structure composed of infiltrated PbS CQDs surrounding a monolayer triangular lattice of latex spheres with diameters of 250 nm or 200 nm, a 250 nm lattice constant, and a slab thickness of 250 nm. (e) The real (blue) and imaginary (orange) components of the refractive index of the CQD material as a function of frequency.

Comparing the case of the non-absorbing PC slab with the case of the CQD-PC with full dispersion, it can be seen that the frequencies of the photonic bands are relatively unchanged with the added dispersion, consistent with our previous study on the effects of dissipation [17]. With the addition of CQD absorption to the model, the clarity of the higher-order bands decreases significantly; this is likely due to the increased absorption that exists at the higher frequencies as well as from the shorter

absorption lengths at higher frequencies present in the model. The rough maintenance of the photonic bands at frequencies with weaker material loss can be understood from using the perturbation theory applied to the PC master equation [10]. Adding a small imaginary part to the dielectric function,  $\epsilon$ , causes the addition of an imaginary part to the resonance frequency,  $\omega_0 = \omega_0 - i\gamma$ , which then adds to the linewidth of the Lorentzian resonance profile and reduces the resonance peak height.

Although there is no complete photonic bandgap, our simulations show evidence for a reduced photonic density of states in the non-absorbing, close-packed (d=250 nm) system near 400 THz, and this feature is largely preserved in the system that includes the full refractive index model for the CQD material. When the latex beads are etched (d=200 nm), the photonic band structure shifts down in frequency, moving the reduced photonic density of states to lower frequencies. This region exhibits smaller absorption, and thus even more of the bands are preserved in this structure.

In-plane photonic bands, in a slab-like PC, directly interact with the external propagating fields, specifically the reflected and transmitted fields, and therefore using them in absorbing materials, such as CQD films, represents a potential spectral tuning mechanism for photovoltaic applications. In PC thin films of interest for such photovoltaic applications, the periodicities are always smaller than the wavelengths of interest; thus, for plan wave sources, no diffraction orders exist. Because of this, all fields and modes that interact with the incident waves can be mapped to the reflected and transmitted waves with the same in-plane wave vector as the incident wave [17]. The in-plane photonic bands correspond to peaks in the transmission and valleys in the reflection spectra, leading to increased absorption near these resonances [17]. Photovoltaics and other optoelectronic applications that rely on the absorption of photoactive materials could potentially benefit from this spectrally-dependent increase in absorption.

Using 2D CQD-PC slabs should enable spectral modulation, including absorption and transmission tuning, through careful control of PC parameters. As seen previously [17], broadband transmission and reflection selectivity is controlled primarily by the optical properties of the slab, such as the refractive index, the volume ratio of the periodic low-index material, and the slab thickness. The locations of the resonant features corresponding to the photonic bands depend on the PC structural properties, such as the periods and shapes of the voids.

The partial preservation of an artificial photonic band structure within a strongly absorbing material such as a CQD film and the existence of a reduced photonic density of states indicates the potential for CQD-PCs to be spectrally-tuned for targeted optoelectronic applications. This could be particularly relevant for photovoltaic applications such as multijunction solar cells, where each cell is responsible for the absorption of a particular portion of the spectrum, while allowing other portions of the spectrum to be transmitted and absorbed by underlying cells.

## IV. SUMMARY

We analyzed a strategy for tuning the spectral selectivity of a thin film absorbing material composed of infrared-responsive PbS CQDs, for photovoltaics and other optoelectronic applications, by using photonic band engineering, where inplane photonic bands are used to control the properties of the out-of-plane transmission and reflection spectra. Using FDTD simulations to artificially vary the imaginary part of the dielectric constant controlling absorptivity, we discovered that a photonic structure formed within a strongly absorbing material, such as PbS CQDs, is able to maintain parts of its photonic band structure, including a reduced photonic density of states in a frequency range of interest. This demonstrates that photonic crystals may prove to be a viable route to achieve spectral selectivity within an absorbing material, useful for photovoltaic applications that require spectral selectivity such as multijunction solar cell and transparent photovoltaics.

Future work will focus on expanding on these results through experimental exploration of other PC structures that could be viable for spectral selectivity. We will use insights gained from this study to design spectrally-selective infrared solar cell materials for multijunction photovoltaics as well as other photoactive optoelectronics. The platform demonstrated here should form the beginning of a new way to approach using photonic band engineering to controls the spectral selectivity of absorbing semiconductor materials.

## REFERENCES

- [1] S. B. Dworkin and T. J. Nye, "Image processing for machine vision measurement of hot formed parts," *J. Mater. Process. Technol*, vol. 174, pp. 1-6, 2006.
- [2] D. Bračun, G. Škulj and M. Kadiš, "pectral selective and difference imaging laser triangulation measurement system for on line measurement of large hot workpieces in precision open die forging," *Int. J. Adv. Manuf. Technol.*, no. 90, p. 917–926, 2017.
- [3] J. J. Talghader, A. S. Gawarikar and R. P. Shea, "Spectral selectivity in infrared thermal detection," *Light Sci. Appl*, vol. 1, p. e24, 2012.
- [4] H. Hara, N. Kishi, M. Noro, H. Iwaoka and K. Suzuki, "Fabry-Perot filter, wavelength-selective infrared detector and infrared gas analyzer using the filter and detector". United States patent Patent US6590710B2, 8 July 2003.
- [5] A. D. Vos, "Detailed balance limit of the efficiency of tandem solar cells," J. Phys. Appl. Phys., vol. 13, p. 839, 1980.
- [6] K. A. Bush, A. F. Palmstrom, Z. J. Yu, M. Boccard, R. Cheacharoen, J. P. Mailoa, D. P. McMeekin, R. L. Z. Hoye, C. D. Bailie, T. Leijtens, I. M. Peters, M. C. Minichetti, N. Rolston, R. Prasanna, S. Sofia, D. Harwood, N. Ma, F. Moghadam, H. J. Snaith and Buonassisi, "23.6%-efficient

- monolithic perovskite/silicon tandem solar cells with improved stability," *Nat. Energy*, vol. 2, p. 17009, 2017.
- [7] H. Kim, H. S. Kim, J. Ha, N. G. Park and S. Yoo, "Empowering semi-transparent solar cells with thermal-mirror functionality," *Adv. Energy Mater.*, vol. 6, no. 1502466, 2016.
- [8] J. C. Knihgt, T. A. Birks, P. S. Russell and D. M. Atkin, "All-silica single-mode optical fiber with photonic crystal cladding," *Opt. Lett.*, vol. 21, p. 1547–1549, 1996.
- [9] E. Kuramochi, K. Nozaki, A. Shinya, K. Takeda, T. Sato, S. Matsuo, H. Taniyama, H. Sumikura and M. Notomi, "Large-scale integration of wavelength-addressable all-optical memories on a photonic crystal chip," *Nat. Photonics*, vol. 8, p. 474–481, 2014.
- [10] J. D. Joannopoulos, S. G. Johnson, J. N. Winn and R. D. Meade, Photonic Crystals: Molding the Flow of Light - Second Edition, Princeton University, 2011.
- [11] J. D. Joannopoulos, P. R. Villeneuve and S. Fan, "Photonic crystals: putting a new twist on light," *Nature*, vol. 386, p. 143–149, 1997.
- [12] A. Mishra and P. Bäuerle, "Small Molecule Organic Semiconductors on the Move: Promises for Future Solar Energy Technology," *Angew. Chem. Int. Ed.*, no. 51, p. 2020– 2067, 2012.
- [13] H. A. Haus, Waves and Firels in Optoelectronics, Englewood Clifs: Prenitce Hall, 1984.
- [14] S. Fan, W. Suh and J. D. Joannopoulos, "emporal coupled-mode theory for the Fano resonance in optical resonators," *J. Opt. Soc. Am*, vol. 20, p. 569, 2003.
- [15] W. Suh, Z. Wang and S. Fan, "Temporal coupled-mode theory and the presence of non-orthogonal modes in lossless multimode cavities," *IEEE J. Quantum Electron*, vol. 40, p. 1511–1518, 2004.
- [16] K. F. Renk and L. Genzel, "Interference Filters and Fabry-Perot Interferometers for the Far Infrared," *Appl. Opt.*, vol. 1, p. 643–648, 1962.
- [17] B. Qiu, Y. Lin, E. S. Arinze, A. Chiu, L. Li and S. M. Thon, "Photonic band engineering in absorbing media for spectrally-selective optoelectronic films," *Opt. Express*, vol. 26, pp. 26933-26945, 2018.
- [18] G. H. Carey, A. L. Abdelhady, Z. Ning, S. M. Thon, O. M. Bakr and E. H. Sargent, "Colloidal quantum dot solar cells," *Chem. Rev.*, vol. 115, p. 12732–12763, 2015.
- [19] E. S. Arinze, B. Qiu, N. Palmquist, Y. Cheng, Y. Lin, G. Nyirjesy, G. Qian and S. M. Thon, "Color-tuned and transparent colloidal quantum dot solar cells via optimized multilayer interference," *Opt. Express*, vol. 25, p. A101–A112, 2017.
- [20] V. Lucarini, J. J. Saarinen, K. E. Peiponen and M. Vartiainen, Kramers-Kronig Relations in Optical Materials Research, Springer Science & Business Media, 2005.
- [21] I. A. Sukhoivanov and I. V. Guryev, Photonic Crystals: Physics and Practical Modeling, Springer Series in Optical Sciences, 2009.